Exact theory of the four-wave-mixing process in a nondissipative medium with a large rate of conversion: Weak-field case

B. Kryzhanovsky
Institute for Physical Research, Armenian Academy of Science, Ashtarak 378410, U.S.S.R.

Boris Glushko
Department of Environmental Sciences and Energy Research, Weizmann Institute of Science, 76 100 Rehovot, Israel
(Received 19 August 1991)

Without making the nondepleted-pump approximation, we solve the problem of four-wave mixing (FWM) in a nondissipative $\chi^{(3)}$ medium. Instead of describing the dynamics of FWM in terms of coupled wave amplitudes, we base our solution on canonical equations that describe the propagation of the field's intensities. This structure clearly identifies the conservative exchange of energy in the FWM process. Consequently, analysis of the FWM process is reduced to a single propagation equation that describes the energy exchange between the pump and amplified waves. This equation yields an elliptic-integral solution. The conversion efficiency reduces to the simple analysis of a fourth-order polynomial, which we analyze to determine the conditions for optimization. The destructive influence of the optical Kerr effect on the phase-matching condition is shown to be eliminated by proper choice of nonzero initial wave-vector mismatch, dependent on the input intensity. The effect of the nonuniform transverse pump-beam intensity profile on the process of conversion is considered. The direction of the energy exchange is shown to be a periodic function of the propagation distance. The transverse intensity distribution of the generating waves provides the characteristic spatial structure (the set of coaxial rings with or without the central spot; the number of rings is explicitly determined by the length of interaction). Several methods of process optimization are discussed, and nonuniformity in the pump-beam profile is shown to be the main reason that complete energy transfer is not achieved.

PACS number(s): 42.65.Ky

I. INTRODUCTION

The four-wave-mixing (FWM) process in nondissipative media has been investigated in a number of works from several different points of view [1–11]. It is well known [12–14] that the process of energy transformation of pump waves (frequencies ω_1 and ω_2) into the energy of amplified waves (frequencies ω_3 and ω_4) is most effective, if the energy-conservation rule $\omega_1+\omega_2=\omega_3+\omega_4$ and momentum-conservation rule, $\mathbf{k}_1+\mathbf{k}_2=\mathbf{k}_3+\mathbf{k}_4$ are met simultaneously. The standard approach to solve these kinds of problems is to expand the value P of the medium polarization, as a power series of the field amplitudes of the interacting waves. Only the terms of lower order are retained:

$$P=\chi^{(1)}E+\chi^{(3)}:EEE\ , \tag{1}$$

where $E=\sum_{j=1}^{4}E_j(\mathbf{r},t)$. Substitution of (1) into the wave equation leads to the well-known system of equations for slowly varying field amplitudes of ω_j waves. The solution of these equations is usually performed by the nondepleted pump-field approach. Using this standard approach, it is difficult to investigate and find the answers for three principal questions.

(1) As the energy in the pump waves (ω_1 and ω_2) is depleted and transferred to the amplified waves (ω_3 and ω_4), how does the FWM process proceed?

(2) Under what conditions can there be a complete transfer of energy from the pump to the probe waves?

(3) How does the optical Kerr effect (i.e., the intensity-dependent index of refraction) disturb the rate of conversion? What can be done to avoid its negative influence?

Only recently have there been considerable efforts to analyze the processes of pump depletion and complete energy transfer [15–17]. It should be mentioned that all these works use the Hamiltonian formalism, proposed first for third-harmonic generation [18]. This formalism enables the conversion of coupled four-wave equations to the simple one-dimensional differential equation describing classical motion in the potential well. Analysis of this equation has shown the principal possibility for complete energy transfer from the pump to the signal waves. The condition of such conversion is the nonzero initial wave-vector mismatch, dependent on the input intensity [16,17,19]. The extension of the problem to noncollinear propagation has been made [19] and an additional scheme to provide appropriate phase-matching condition suggested (by proper choice of angular mismatch). The influence of the pulse temporal profiles on the efficiency of conversion has been also taken into account. The nonuniform intensity distribution of the pulses results in the decreasing of the whole rate of conversion, since now the ideal phase-matching condition can be performed for the local part of the pulse only.

In the present work we consider the influence of the spatial profile of interacting pulses on the process of complete energy transfer. In Secs. II and III we follow mainly the Hamiltonian approach used in a previous work [19]. The approach is based on the representation of medium polarization P as a partial derivative [14,18–20],

$$P=-\frac{\partial H}{\partial E}\ , \tag{2}$$

where H is the part of the Hamiltonian describing the interaction of the field with the medium (in other words, H is part of the time-averaged free-energy density of a dielectric [1]). Under this representation the propagation equations for the slowly varying amplitudes of the interacting waves have the same form as the canonical Hamiltonian equations. This enables the use of a completely developed classical-mechanical technique: The four independent integrals of motion can be easily obtained, reducing the problem to the solution of one differential equation [see Eq. (21), below], which describes pendulum oscillations in classical mechanics. This equation takes into account both $\omega_1+\omega_2\rightarrow\omega_3+\omega_4$ and $\omega_3+\omega_4\rightarrow\omega_1+\omega_2$ energy-transformation channels, as well as the interference between them. In a nondissipative media, the polarization responds instantaneously to changes in the field; i.e., the adiabatic following the regime is attained. In the interest of simplicity and clarity, we consider the weak-field case only. However, the approach proposed here may be used for arbitrary field intensities.

Usually, the negative influence of the optical Kerr effect is related to the variation of the wave-vector mismatch, $\Delta\mathbf{k}=\mathbf{k}_1+\mathbf{k}_2-\mathbf{k}_3-\mathbf{k}_4$, during the conversion process and the regime of complete phase matching ($\Delta\mathbf{k}=0$) cannot be performed in principle. However, as shown below, such variation of $\Delta\mathbf{k}$ does not disturb the FWM-process optimization and the negative Kerr effect influence can be completely eliminated by the proper nonzero choice of the initial $\Delta\mathbf{k}_0$ value. The main difficulties of the FWM-process optimization are related to the nonuniformity of the transverse spatial-intensity distribution of the pump waves, which makes it impossible to choose the proper initial $\Delta\mathbf{k}_0$ value which applies to the entire beam cross section.

This work is organized as follows: In Sec. II the wave equations are reduced to the canonical Hamiltonian form and the free energy is shown not to be the motion integral. In Sec. III four motion integrals (13) are obtained, which allows the exclusion of all the variables but one from consideration. In Sec. IV the FWM problem is reduced to one differential equation and its explicit solution is obtained. In Sec. V this explicit solution is analyzed for the most important case, when only three input waves are considered (the same case is analyzed in the following sections) and condition (37) for the initial Δk_0 value, under which the conversion efficiency is maximized, is obtained. In Sec. VI the quantum conversion efficiency is considered and general ways to optimize this value are shown. In Secs. VII and VIII some particular limiting cases are considered.

II. FORMULATION OF THE PROBLEM: WAVE EQUATIONS

We consider the propagation process of FWM in a medium which fills the semispace $z\geq 0$. It is supposed that carried frequencies ω_j of the plane wave E_j ($j=1,2,3,4$) satisfy the energy-conservation condition $\omega_1+\omega_2=\omega_3+\omega_4$. The input beam angles with respect to the z axis, θ_j, are assumed to be small enough ($\theta_j \ll 1$) to omit the vector signs of the amplitudes $\mathbf{E}_j$ and to consider the scalar equations. We also suppose that the values of the refractive indices are close to unity $[|n(\omega_j)-1|\ll 1]$. It will be shown further that the results obtained can be extended to cases where the last condition does not apply. The wave amplitudes are

$$E_j(\mathbf{r},t)=E_j\exp(i\mathbf{k}_{j0}\cdot\mathbf{r}-i\omega_j t)+\text{c.c.}\ , \tag{3}$$

where E_j is a slowly varying function of the variables z, $\tau=t-z/c$ and $\mathbf{k}_{j0}$ is the input wave vector at the entrance of the medium ($|\mathbf{k}_{j0}|=\omega_j/c$). The true values of $\mathbf{k}_j$ in the medium are functions of the z coordinate and include an intensity-dependent Kerr effect. Following [1], the H value is determined from

$$-H=\sum_j\chi^{(1)}(\omega_j)|E_j|^2+\tfrac{1}{2}\sum_{ij}B_{ij}|E_kE_j|^2 +[\chi^{(3)}_{\text{FWM}}E_1E_2E_3^*E_4^*\exp(iqz)+\text{c.c.}]\ , \tag{4}$$

where q is the projection of the $\mathbf{q}$ vector on the z axis,

$$\mathbf{q}=\mathbf{k}_{10}+\mathbf{k}_{20}-\mathbf{k}_{30}-\mathbf{k}_{40}\ , \tag{5}$$

and $\chi^{(1)}(\omega_j)$ are the linear susceptibilities at frequency ω_j; $\chi^{(3)}_{\text{FWM}}=\chi^{(3)}(-\omega_4,\,\omega_1,\,\omega_2,\,\omega_3)$ is the nonlinear third-order susceptibility, responsible for the FWM; $B_{ij}=\frac{1}{2}\chi^{(3)}(-\omega_i,\,\omega_i,\,\omega_j,\,-\omega_j)$ are the diagonal elements of the nonlinear third-order susceptibility, which is responsible for the nonlinear terms of the refractive index. The refractive index at ω_j is written as

$$n_j=1+2\pi\chi^{(1)}(\omega_j)+4\pi\sum_{m=1}^{4}B_{jm}|E_m|^2\ . \tag{6}$$

According to Eq. (2), the medium polarization is written as

$$P=\sum_j\left[\frac{\partial H}{\partial E_j^*}\exp(i\mathbf{k}_{j0}\cdot\mathbf{r}-i\omega_j t)+\text{c.c.}\right]\ . \tag{7}$$

Substitution of Eq. (7) into the wave equation for slowly varying amplitudes leads to a coupled system of equations for E_j:

$$\frac{dE_j}{dz}=-i\frac{2\pi\omega_j}{c}\frac{\partial H}{\partial E_j^*}\ . \tag{8}$$

In order to solve Eq. (8), we rewrite it in terms of the intensity I_j and phase ψ_j:

$$E_j=|E_j|e^{i\psi_j},\quad I_j=c|E_j|^2/2\pi\hbar\omega_j\ . \tag{9}$$

The Hamiltonian H in these variables takes the form

$$\frac{1}{\hbar}H=-\sum_{j}\gamma_j I_j-\sum_{j,k}b_{jk}I_jI_k-\chi\sqrt{I_1I_2I_3I_4}\cos\psi\ , \quad (10)$$

where

$$\psi=\psi_4+\psi_3-\psi_2-\psi_1-\psi_\chi-qz\ ,$$
$$\gamma_j=2\pi\omega_j\chi^{(1)}(\omega_j)/c\ , \quad (11a)$$
$$b_{jk}=(2\pi/c)^2\hbar\omega_j\omega_k B_{jk}\ ,$$
$$\chi=2\hbar(2\pi/c)^2|\chi^{(3)}_{\rm FWM}|\sqrt{\omega_1\omega_2\omega_3\omega_4}\ . \quad (11b)$$

Here ψ_χ is the phase of $\chi^{(3)}_{\rm FWM}$. The canonical transformation (9) of Eq. (8) gives the following expressions for a new pair of conjugative variables I_j and ψ_j:

$$\frac{dI_j}{dz}=\frac{1}{\hbar}\frac{\partial H}{\partial\psi_j},\quad \frac{d\psi_j}{dz}=\frac{-1}{\hbar}\frac{\partial H}{\partial I_j}\ . \quad (12)$$

In the case of a noncollinear ($q\neq0$) interaction, Eq. (12) describes a nonconservative system, i.e., $\partial H/\partial z\neq0$. It is obvious that the free energy varies with z, because of energy redistribution between the quantum beams propagating at different angles with respect to each other (the resulting Poynting vector changes its direction). Consequently, the role of the Hamiltonian will play another magnitude signed as H_0 and determined below [Eq. (16)].

III. MOTION INTEGRALS

Analyzing Eq. (10), one realizes that $\partial H/\partial\psi_1=\partial H/\partial\psi_2=-\partial H/\partial\psi_3=-\partial H/\partial\psi_4=\partial H/\partial\psi$. Substitution of these relations into Eq. (12) results in four independent integrals of motion:

$$I_1-I_2=I_{10}-I_{20},\quad I_3-I_4=I_{30}-I_{40}\ ,$$
$$I_1+I_2+I_3+I_4=I_{10}+I_{20}+I_{30}+I_{40}\ , \quad (13a)$$

and

$$H-\frac{q}{4}(I_1+I_2-I_3-I_4)=H(z=0)-\frac{q}{4}(I_{10}+I_{20}-I_{30}-I_{40})\ , \quad (13b)$$

where $I_{j0}=I_j(z=0)$ and $H(z=0)$ are the initial values of I_j and H. Equations (13a) are known as the Manly-Rowe relations [21] and are widely used in the theory of parametric amplification [22]. The relation (13b) describes the $H(z)$ behavior. It follows from (13b) that only in the case $q=0$ does the free energy H not depend on z. The relations (13a) in turn enable a reduction of the four variables I_j to one, I:

$$I_1=I_{10}-I,\quad I_2=I_{20}-I\ ,$$
$$I_3=I_{30}+I,\quad I_4=I_{40}+I\ . \quad (14)$$

The magnitude of I is characteristic of the energy exchange between waves $\omega_{1,2}$ and $\omega_{3,4}$: The initial condition for $I(z)$ is $I(0)=0$.

The next step of our mathematical formalism is to reduce four pair conjugative variables I_j,ψ_j to new ones. The variables I and ψ are chosen as one of the pairs; the choice of the other three pairs does not really play a role. Then Eq. (12) is written as

$$\frac{dI}{dz}=-\frac{1}{\hbar}\frac{\partial H_0}{\partial\psi},\quad \frac{d\psi}{dz}=\frac{1}{\hbar}\frac{\partial H_0}{\partial I}\ , \quad (15)$$

where

$$H_0=H+\hbar qI\ . \quad (16)$$

It is readily noted that Eqs. (15) have the same form as the canonical Hamiltonian equations for one-dimensional classical motion. The values I and ψ are regarded as the generalized coordinate and momenta, respectively, the z-variable replaces the time, and $H_0/\hbar$ is equivalent to the Hamiltonian. It is seen from Eqs. (10) and (16) that H_0 has no explicit z dependence. It is consequently the fourth motion integral, i.e., $dH_0/dz=0$, which results in conservation of the energy density of the medium along the z axis. The expression for H_0 can be written as an explicit function of I and ψ. Substituting Eq. (14) into (16), we obtain H_0 as a function of variables I and ψ only:

$$-\frac{1}{\hbar}H_0=(\Delta k_0+bI)I-\chi f\cos\psi\ . \quad (17)$$

Here the constant term which does not include the variables I and ψ is omitted. Taking into account the trivial relation $H(z=0)=H_0$, we rewrite Eq. (13) in a form which determines the relationship between phase ψ and intensity I variables:

$$\Delta k_0 I+bI^2=\chi f\cos\psi-\chi f_0\cos\psi_0\ , \quad (18)$$

where

$$\Delta k_0=q+\gamma_1+\gamma_2-\gamma_3-\gamma_4+2\sum_{j=1}^{4}(b_{1j}+b_{2j}-b_{3j}-b_{4j})I_{j0}\ , \quad (19a)$$

$$b=2(b_{13}+b_{14}+b_{42}+b_{32}-b_{12}-b_{34})-b_{11}-b_{22}-b_{33}-b_{44}\ , \quad (19b)$$

$$f=[(I_{10}-I)(I_{20}-I)(I_{30}+I)(I_{40}+I)]^{1/2}\ . \quad (19c)$$

Here $f_0=(I_{10}I_{20}I_{30}I_{40})^{1/2}$ and $\psi_0=\psi(z=0)$.

Because of its importance, let us examine the physical meaning of the value of Δk_0. We determine the wave-vector mismatch Δk as a projection of $\Delta\mathbf{k}=\mathbf{k}_1+\mathbf{k}_2-\mathbf{k}_3-\mathbf{k}_4$ onto the z axis, where $k_j=\omega_j n(\omega_j)/c$. Then, taking into account Eqs. (6) and (19b), we obtain

$$\Delta k=\Delta k_0+2bI\ . \quad (20)$$

As seen, the magnitude $2bI$ defines the exchange of the wave-vector mismatch Δk along the z axis, while Δk_0 is the initial wave-vector mismatch value, i.e., $\Delta k_0=\Delta k(z=0)$.

IV. MOTION EQUATIONS: EXACT SOLUTION

Here Eq. (15) is considered. The first part of Eq. (15) together with Eq. (17) yields the form $dI/dz=\chi f \sin\psi$. Substituting the value of $\sin\psi$ from Eq. (18), we finally obtain

$$\frac{dI}{dz}=\pm\chi\sqrt{V(I)}\ , \tag{21}$$

where

$$V(I)=(I_{10}-I)(I_{20}-I)(I_{30}+I)(I_{40}+I) -\alpha[I^2+(\Delta k_0/b)I+\chi f_0\cos\psi_0/b]^2\ . \tag{22}$$

The sign of Eq. (21) depends on the sign of $\sin\psi_0$, and $\alpha=b^2/\chi^2$ is a dimensionless parameter describing the ratio between diagonal and nondiagonal elements of the $\chi^{(3)}$ susceptibility [see (11) and (19)]. Equation (21) describes one-dimensional finite motion. Such types of equations are widely investigated in the theory of elliptic functions [23–25]. The allowed range of motion of determined by the roots of the equation $V(S)=0$. We indicate these roots as S_j $(j=1,2,3,4)$ and set them as

$$\frac{1}{S_1}\geq\frac{1}{S_2}\geq\frac{1}{S_3}\geq\frac{1}{S_4}\ . \tag{23}$$

In this case I ranges between $S_1\geq I\geq S_4$. One can see from (22) that the roots S_1 and S_4 satisfy the relations

$$I_{10,20}\geq S_1\geq 0\geq S_4\geq -I_{30,40}\ . \tag{24}$$

These relations mean that the direction of energy exchange alters its sign, usually before depletion for any of the input waves occurs. The maximal rate of conversion (i.e., complete depletion for one of the input waves) is achieved only in the case when the initial wave-vector mismatch is taken as

$$\Delta k_0=-bI_{\min}-\chi f_0\cos\psi_0/I_{\min}\ . \tag{25}$$

When condition (25) holds, we obtain $S_1=I_{\min}$, if $I_{\min}=\min\{I_{10},I_{20}\}$, or $S_4=-I_{\min}$, if $I_{\min}=\min\{I_{30},I_{40}\}$. In order to obtain the value of Δk_0 in the form of Eq. (25), one should properly choose the input beam angles θ_j. It should be mentioned that as the condition for maximal conversion, Eq. (25) is not sufficient. In order to make it so, we should require the value $I_{\min}$ to be the least positive root of Eq. (22).

The general solution of Eq. (21) is given by

$$I(z\pm L)=S_1\frac{\mathrm{sn}^2(gz/\mu)}{1+\nu\,\mathrm{cn}^2(gz/\mu)}+S_4\frac{(1-\nu)\mathrm{cn}^2(gz/\mu)}{1+\nu\,\mathrm{cn}^2(gz/\mu)}\ ,$$

where $\mathrm{sn}(x/\mu)$ and $\mathrm{cn}(x/\mu)$ are the Jacobian elliptic functions (elliptic sine and cosine, respectively); the parameters μ and ν are given by

$$\mu=\frac{(S_1-S_4)(S_2-S_3)}{(S_1-S_3)(S_2-S_4)},\quad \nu=\frac{S_1-S_4}{S_4-S_3}\ , \tag{27}$$

and satisfy the condition $1\geq\mu\geq0$ and $\nu\geq0$; the gain g is written as

$$g=\tfrac{1}{2}\chi\sqrt{(1-\alpha)(S_1-S_3)(S_4-S_2)}\ . \tag{28}$$

The length L is defined as $L=F(\xi,\mu)/g$, where $F(\xi,\mu)$ is a second-order elliptic integral with parameter μ and variable $\xi=\sqrt{S_4(S_1-S_3)/S_3(S_4-S_2)}$.

Expression (26) describes the periodical function $I(z)=I(z+2l)$; i.e., the direction of energy transfer changes its sign with the period $2l$ (see Fig. 1). The half-period value l is given by

$$l=K(\mu)/g\ , \tag{29}$$

where $K(\mu)$ is the full first-order elliptic integral. The function $K(\mu)$ has been tabulated [26,27]. However, the relation of Tricomi [28], $\ln 4\leq K(\mu)+\frac{1}{2}\ln(1-\mu)\leq\pi/2$, allows us to obtain an extremely convenient estimation for l:

$$\frac{1}{2g}\ln\frac{e^{\pi}}{1-\mu}\geq l\geq\frac{1}{2g}\ln\frac{16}{1-\mu}\ . \tag{30}$$

Using either the left side of Eq. (30) for $0\leq\mu\lesssim0.6$ or the right side for $0.6\lesssim\mu\leq1$ allows one to estimate l with a relative error of less than 3%. As seen from Eq. (30), $l\to\infty$ for strong convergence of some roots $S_j(\mu\to1)$. In this case the function $I(z)$ becomes nonperiodic and the energy-transfer direction either does not change its sign at all or changes sign only once at $z=L$ [see Figs. 1(b) and 1(c)]. The case $l\to\infty$ is a pure mathematical abstraction, since it can be obtained only for definite values of input intensities I_{j0} and wave-vector mismatch Δk_0. The solution with $l=\infty$ is extremely unstable; i.e., any small deviation of the variables mentioned above makes the l value finite and comparable in magnitude

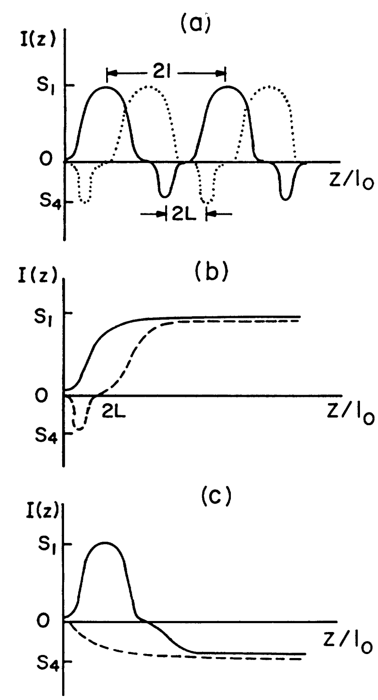

FIG. 1. Intensity $I(z)$ vs normalized distance z/l_0 for $\sin\psi_0>0$ (solid line) and $\sin\psi_0<0$ (dashed line): (a) without degeneracy of roots S_j, (b) $S_1=S_2$, and (c) $S_3=S_4$.

with g^{-1}. The estimations show that in most cases of interest l varies within the limits $2g^{-1} \le l \le 10g^{-1}$.

V. SOLUTION FOR $I_{40}=0$: GENERAL EXPRESSIONS

From here on we consider the case of practical application, $I_{40}=0$. Under this condition Eq. (14) shows that the magnitude I equals the intensity I_4. The function $V(I)$ takes the form $V(I)=IR(I)$, where

$$R(I)=(I_{10}-I)(I_{20}-I)(I_{30}+I)-\alpha I(I+\Delta k_0/b)^2 \,. \tag{31}$$

The values $S_1^{-1} \ge S_2^{-1} \ge S_3^{-1}$ are determined from the roots of Eq. (31), $S_4=0$, respectively. The magnitude I in this case varies between 0 and S_1, and its dependence on z is given by the expression

$$I(z)=S_1\frac{\mathrm{sn}^2(gz/\mu)}{1+\nu\,\mathrm{cn}^2(gz/\mu)}\,, \tag{32}$$

where

$$\nu=-\frac{S_1}{S_3},\quad \mu=\frac{1-S_3/S_2}{1-S_3/S_1}\,,$$
$$g=\frac{1}{2}\chi\left[I_{10}I_{20}I_{30}\left[\frac{1}{S_1}-\frac{1}{S_3}\right]\right]^{1/2}. \tag{33}$$

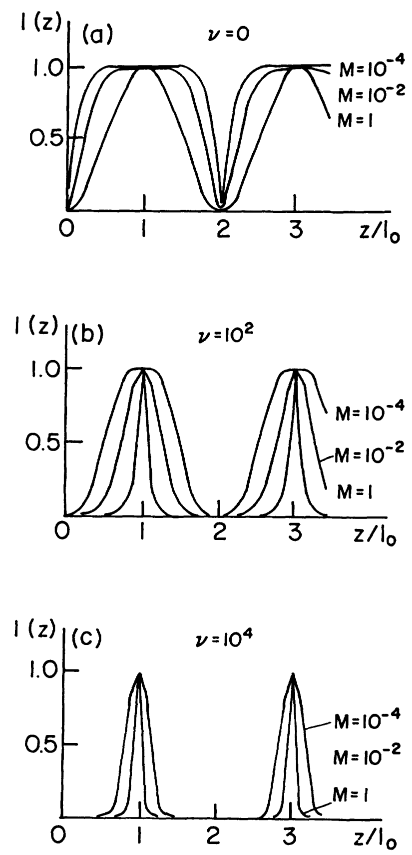

FIG. 2. Intensity $I(z)$ vs normalized distance z/l_0 for the various values of the parameters ν and $M=1-\mu$, in the case $I_{40}=0$.

The dependence of $I(z)$ for different values of the parameters μ and ν is shown in Fig. 2. Now we consider several cases, where the roots S_j ($j=1,2,3,4$) are degenerate.

(1) $S_1=S_2$. In this case ($\mu=1$), $l=\infty$, the function $\mathrm{sn}(x/\mu)$ transfers into the hyperbolic tangent $\mathrm{sn}(x/1)=\tanh x$, and Eq. (32) becomes

$$I(z)=S_1\frac{\sinh^2 gz}{\nu+\cosh^2 gz}\,. \tag{34}$$

(2) $S_2=S_3$. In this case ($\mu=0$), the imaginary period of $\mathrm{sn}(x/\mu)$ becomes infinite, i.e., $\mathrm{sn}(x/0)=\sin x$, and Eq. (32) takes the form

$$I(z)=S_1\frac{\sin^2 gz}{1+\nu\cos^2 gz}\,. \tag{35}$$

(3) $S_1=S_2=S_3$. This situation is realized when the following condition holds: $A=[I_{30}(I_{10}+I_{20})-I_{10}I_{20}+\Delta k_0^2/\chi^2]>0$. In this case $l=\infty$, and Eq. (32) takes the form

$$I(z)=\frac{1}{4}I_{10}I_{20}I_{30}\frac{\chi^2z^2}{1+A\chi^2z^2}\,. \tag{36}$$

Expressions (34)–(36) illustrate the root's exact degeneracy. However, these expressions can be utilized for the estimation process in the cases where exact degeneracy is absent. For instance, when $\mu \lesssim 0.6$ the function $\mathrm{sn}(x/\mu)$ is slightly different from $\sin x$. Therefore expression (35) with the substitution $gz \to \pi z/2l$ describes $I(z)$ with sufficient accuracy. Similarly, for $\mu \gtrsim 0.6$ expression (34) can be utilized within the half period $0 \le z \le l$. The cases (34)–(36) are shown graphically in Fig. 3.

Now we consider the efficiency of energy transfer into the wave ω_4. As was mentioned, the maximal value of the ω_4-wave intensity is equal to S_1 and is reached for $z=(2m+1)l$, where $m=0,1.\ldots$ Thus conversion-efficiency analysis in the plane-wave approach is reduced to the analysis of the magnitude of S_1, the least positive root of Eq. (31), $R(S)=0$. For simplicity, we take the case $I_{20} \ge I_{10}$. Then the local conversion efficiency can be determined as $\eta=S_1/I_{10}$ (the meaning of "local" efficiency is explicitly defined in Sec. VI). The maximal conversion $\eta=1$ occurs under complete depletion of the ω_1 wave. From (25) and (31), the value $S_1=I_{10}$, i.e., $\eta=1$ can be reached only by proper choice of initial wave-vector mismatch Δk_0,

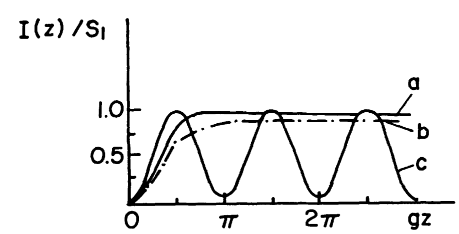

FIG. 3. Normalized $I(z)/S_1$ vs normalized distance gz for the cases of S_j root degeneracy: (a) $S_1=S_2$, (b) $S_1=S_2=S_3$, and (c) $S_3=S_4$.

$$\Delta k_0 = -bI_{10} \ . \tag{37}$$

The physical meaning of condition (37) is elucidated by considering the average value $\langle \Delta k \rangle$, which is determined as follows:

$$\langle \Delta k \rangle = \frac{1}{S_1}\int_0^{S_1} \Delta k(I)dI = \Delta k_0 + bS_1 \ . \tag{38}$$

We realize immediately from (38) that $\langle \Delta k \rangle = 0$ if condition (37) holds. Thus we maintain that the negative influence of the intensity-induced Kerr effect can be completely eliminated (in the plane-wave approach) by taking the initial Δk_0 in the form of Eq. (37). The sign of $\Delta k(z)$ changes periodically [$\Delta k = \Delta k_0$ for $z = 2ml$ and $\Delta k = -\Delta k_0$ for $z = (2m+1)z$, where $m = 0, 1 \ldots$], while the average value of $\Delta k(z)$ is equal to zero.

VI. QUANTUM CONVERSION EFFICIENCY

In this section we consider the quantum conversion efficiency (QCE) $W = W(z)$, which we define as the ratio between the photon number in the ω_4 wave and the initial photon number in the ω_1 wave. Supposing axial-beam symmetry, we can write the following expression for W:

$$W = \left[\int_0^\infty I_\rho \, d\rho\right] \Big/ \left[\int_0^\infty I_{10}\rho \, d\rho\right] , \tag{39}$$

where ρ is a transverse coordinate. All previous considerations relating to the conversion efficiency are valid, generally speaking, in the monochromatic plane-wave approach, i.e., large pump-beam radius and uniform transverse-intensity distribution: thus one can put $I_{j0}(\rho) =$ const. In this case the $W(z)$ dependence coincides exactly with $I(z)$; the optimal condition (37) applies to the whole beam cross section, leading consequently to the maximal rate of conversion, $W = 1$, at distances $z = (2m+1)l$ ($m = 0, 1 \ldots$). In a real situation the pump-beam transverse-intensity distribution is nonuniform. Although the plane-wave approach is still valid from the mathematical point of view, the nonuniform intensity dependence along with the radius ρ should be taken into account.

The radial $I_{j0}(\rho)$ dependence means that all the parameters involved, g, l, Δk_0, and η, become functions of the coordinate ρ. The dependence $\Delta k_0 = \Delta k_0(\rho)$, for instance, means that the optimal condition (37) cannot hold simultaneously along the whole beam cross section: i.e., the maximal efficiency $W = 1$ cannot in principle be achieved. The transformation "period" dependence $l = l(\rho)$ means that different parts of the beam cross section have different rates of conversion; moreover, they can have opposing directions of energy exchange ($\omega_1 + \omega_2 \rightleftarrows \omega_3 + \omega_4$). In such conditions the magnitude $\eta = \eta(\rho)$ indicates the conversion rate for different parts of the beam cross section, depending on the distance ρ from the beam axis.

In most experiments performed, a sufficiently low quantum conversion efficiency is obtained ($W \ll 1$). This fact is usually related to the negative influence of the optical Kerr effect. It is natural that the Kerr effect lead to a decrease of the conversion efficiency. However, in some cases its negative influence can be more or less eliminated (see Secs. VIII and IX). We show below that the main factor which strongly decreases the efficiency is the pump intensity-dependent period l of the energy transfer.

The discussion below is divided into two cases: the absence of the Kerr effect and the more general Kerr active-medium case.

(a) When the Kerr effect is absent, $b = b_{ij} = 0$. Consider the case where the exact phase-matching condition $\Delta k_0 = 0$ occurs. Suppose that the pump beams are coaxial and have the same transverse distribution:

$$I_{j0}(\rho) = I_{j0}(0)e^{-(\rho/\rho_0)^2} \ . \tag{40a}$$

Now $l(\rho)$ will take the form

$$l = l_0 \exp(\rho/\rho_0)^2 \ , \tag{40b}$$

where l_0 is the minimal value of the transfer period, at the pump-beam center ($\rho = 0$). As follows from Eq. (32), for $z < l_0$ the energy transfer of any part of the pump occurs in the same way, $\omega_1 + \omega_2 \to \omega_3 + \omega_4$. For lengths $z > l_0$, some parts of the pump experience the opposite direction of transfer, $\omega_3 + \omega_4 \to \omega_1 + \omega_2$. Therefore the ω_4-wave transverse-intensity distribution obtains the characteristic structure $I = I(z, \rho)$; this dependence is modified with the length z of propagation (Fig. 4). It is readily noted that the transverse-intensity distribution of the ω_4 wave represents a set of coaxial rings with a central spot (or without it). The central spot appears at $z = (2m+1)l_0$ and disappears (by transformation into the new ring) at $z = 2ml_0$, where $m = 0, 1 \ldots$. Thus the

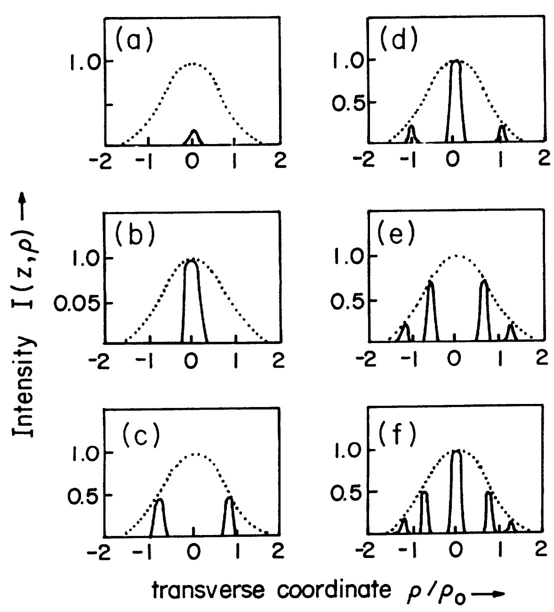

FIG. 4. I_4-beam transverse-intensity distribution vs normalized radius ρ/ρ_0 for various propagation distances: (a) $z = 0.8l_0$, (b) $z = l_0$, (c) $z = 2l_0$, (d) $z = 3l_0$, (e) $z = 4l_0$, and (f) $z = 5l_0$. The curves are calculated using $\Delta k_0 = 0$, $\nu = 10^3$, and $\mu = 0.99$ (dashed line shows the pump-intensity distribution); l_0 is the period of energy transfer at the beam center ($\rho = 0$).

number of rings n is determined by the integer part of the expression $n=[z/2l_0]$. The ring side grows up with enlarging propagation length; the kth ring radius can be determined from Eq. (40):

$$\rho_k=\rho_0[\ln(z/2kl_0)]^{1/2}\ , \tag{41}$$

where $1\le k\le n$. The fact that for $z>l_0$ the energy transfer for the different parts of the beam occurs in different ways shows that it is in principal impossible to perform the complete energy transfer from the ω_1 wave. This result shows that even under idealized conditions ($\Delta k_0=0$ and $b_{ij}=0$), which lead to a maximal conversion rate $\eta(\rho)=1$ for the whole beam, the quantum conversion efficiency $W(z)$ will be less than unity.

Consider now the magnitude $W(z)$. From Eqs. (32), (39), and (41), we obtain

$$W(z)=\frac{\eta}{g_0z}\int_0^{g_0z}\frac{\mathrm{sn}^2(x/\mu)}{1+\nu\,\mathrm{cn}^2(x/\mu)}dx\ , \tag{42}$$

where $g_0=g(\rho=0)$ is the gain value at the pump-beam center. Since the function being integrated is periodic in x, the $W(z)$ dependence has an oscillatory character (Fig. 5). For $z=l_0,3l_0,\dots$, $W(z)$ takes the value W_∞ that it has at $z\to\infty$:

$$W_\infty=\eta[2\Pi_1(\nu',\mu)-\pi]/\pi\nu\ . \tag{43}$$

Here $\Pi_1(\nu',\mu)$ is a full elliptic integral of the third kind with parameter μ and characteristic $\nu'=\nu/(\nu+1)$ [23–25]. As seen from Fig. 5, $W(z)$ reaches its maximum $W_{\max}$ at the first maxima for $z\cong(1.2\pm0.2)l_0$. The dependence of $W_{\max}$ and W_∞ on parameters μ and ν is shown in Fig. 6. As in most cases considered, the conversion efficiency is sufficiently low. The maximal conversion $W_{\max}\sim1$ can be expected in the narrow interval of the parameters μ and ν with strong convergence S_1 and S_2 roots, when $\mu\to1$. It will be seen further that such a situation ($\mu\to1$) is possible in the case of the pump degeneration $I_{10}\to I_{20}$ only. Since we considered the case $\Delta k_0=0$, $b_{ij}=0$, the magnitude $\eta=1$ should be put into Eqs. (42) and (43) (as has been done for Figs. 5 and 6). W dependence similar to Figs. 5 and 6 has been observed in an experiment [29] where conditions allowed a sufficiently high ($W_\infty\sim0.25$) conversion efficiency.

(b) Now we discuss the more general Kerr active-medium case ($b_{ij}\neq0$). The value Δk_0 [Eq. (19a)] can be expressed as a sum of linear ($\Delta k_L=q+\gamma_1+\gamma_2-\gamma_3-\gamma_4$) and nonlinear components. Suppose for simplicity that phase-matching conditions are fulfilled in the linear approximation, i.e., for $\Delta k_L=0$. It is readily seen that in this case the main results of (a) above are still valid, if $\eta=\eta_0$ is taken in Eqs. (42) and (43) and all the curves of Figs. 5 and 6 are normalized to the value η_0, where $\eta_0=\eta$ ($\rho=0$) is the local conversion efficiency at the center of the pump beams. The extent to which $\eta_0<1$ is a measure of the degree that the Kerr effect reduces the conversion efficiency [in addition to the factor considered earlier in (a) above].

The quantum efficiency-optimization procedure has been reduced to optimization of the magnitude of η_0. This may be done by one of two basic approaches. The first one consists of the optimization of η_0 by means of the proper choice of the input intensities I_{j0}. The second is related to the proper choice of the medium and field parameters, under which $b=0$. The large number of independent parameters does not allow us to make more specific comments. Therefore, in the following section, we consider some particular cases.

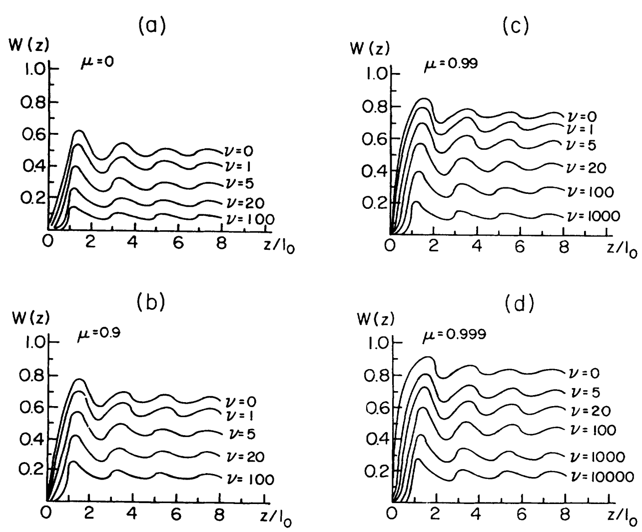

FIG. 5. Quantum conversion efficiency $W(z)$ for several values of the parameters ν and μ: (a) $\mu=0$, (b) $\mu=0.9$, (c) $\mu=0.99$, and (d) $\mu=0.999$. The curves correspond to the conditions of Sec. VI ($b=b_{ij}$).

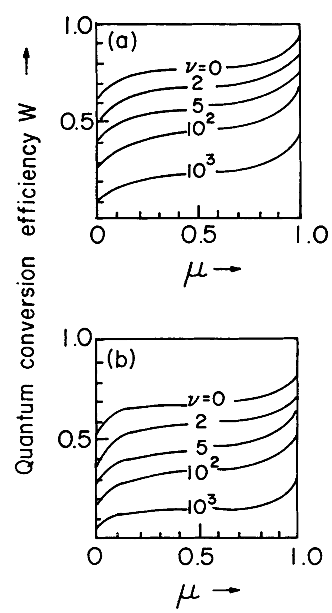

FIG. 6. Quantum conversion-efficiency W dependence on the value of the parameter μ for different values of the parameter $\nu=0,2,5,10^2,10^3$. (a) $W_{\max}$ and (b) W_∞.

VII. SOLUTION FOR THE PARTICULAR CASE $I_{10,20} \gg I_{30}$

Here the gain g has a well-known expression

$$g=(\beta^2-\tfrac{1}{4}\Delta k_0^2)^{1/2}\ , \tag{44}$$

where $\beta=\frac{1}{2}\chi\sqrt{I_{10}I_{20}}$ is the parametric coupling coefficient. The values S_j $(j=1,2,3,4)$ are readily obtained. For instance, $S_3=-I_{30}\beta^2/g^2$, while $S_{1,2}$ are determined as roots of the following equation [see (22)]:

$$(S-I_{10})(S-I_{20})-\alpha(S+\Delta k_0/b)^2=0\ . \tag{45}$$

In the limit considered, $|S_{1,2}| \gg |S_3|$; the parameters μ and ν satisfy the relations $\nu \gg 1$ and $1-\mu \ll 1$. Since the function $I(z)$ is periodic and symmetric with respect to its extrema, we can analyze it within the semiperiod $0 \le z \le l$. Using the asymptotic representation of the function $\mathrm{sn}(x/\mu)$, valid for $\mu \to 1$ [20–22], we obtain, from Eq. (32),

$$I(z)=\frac{S_1|S_3|\sinh^2 gz}{S_1+|S_3|\cosh^2 gz}\ . \tag{46}$$

For the short propagation length, $z \ll l_s = g^{-1}\ln|S_1/S_3|$, Eq. (46) takes a form similar to the well-known expressions (see for instance [2–5]) which have been obtained in the nondepleted-pump-beam approach:

$$I(z)=I_{30}(\beta^2/g^2)\sinh^2 gz\ . \tag{47}$$

The magnitude l_s characterizes the saturation of the conversion process. In most cases the relation $l_s \cong l$ holds, so that the nondepleted-pump-beam approach and expression (47) are valid within the entire region $0 \le z \le l$. A significant difference occurs in the case of strong S_1 and S_2 magnitude convergence, i.e., $|S_1-S_2| \lesssim I_{30}$. In this situation $l_s < l$ and the nondepleted-pump approach is valid for $0 \le z \le l_s$ only; when $z > l_s$ the magnitude $I(z)$ practically reaches its maximal value S_1 with the simultaneous saturation of the conversion process.

In order to consider the general dependence of local conversion efficiency η on the medium and pump-field parameters, we can obtain S_1 from Eq. (45) and substitute it into the expression $\eta=S_1/I_{10}$. Below we consider three important particular cases.

(i) $b=0$ (passive Kerr medium). The conversion process evolves with permanent wave-vector mismatch $\Delta k=\Delta k_0$. The magnitude η is defined as

$$\eta=\frac{I_{10}+I_{20}-[(I_{10}-I_{20})^2+4I_{10}I_{20}\Delta k_0^2/\beta^2]^{1/2}}{2I_{10}}\ . \tag{48}$$

Maximum conversion efficiency is reached under complete phase matching $\Delta k_0=0$.

(ii) $b\ne 0$, $\Delta k_0=0$. The FWM process develops with the increase of the wave-vector mismatch, which becomes equal to $\Delta k(l)=-bS_1$ at the point of maximum conversion. The rate of conversion is characterized by the largest magnitude of the amplification rate $g=\beta$:

$$\eta=\frac{I_{10}+I_{20}-[(I_{20}-I_{10})^2+4\alpha I_{10}I_{20}]^{1/2}}{2I_{10}(1-\alpha)}\ . \tag{49}$$

The maximum rate $\eta=1$ can be achieved for $\alpha=0$ only. With increasing α, the negative influence of the optical Kerr effect arises, which leads to phase mismatch of the interacting waves and, correspondingly, to decreased conversion. However, in the case $I_{20} \gg I_{10}$, the rate of decrease is negligible and η is close to unity, even at large values of α.

(iii) $b\ne 0$, $\Delta k_0=-bI_{10}$. This is the optimal case (37), when the average value of $\langle \Delta k \rangle$ is equal to zero. The conversion efficiency in this case is maximal $\eta=1$, and the amplification rate is equal to

$$g=\beta\sqrt{1-\alpha I_{10}/I_{20}}\ . \tag{50}$$

We see from (50) that process evolution is possible only when $I_{20} > \alpha I_{10}$. As follows from Eqs. (48–50) the case $I_{20} \gg I_{10}$ is required to obtain the large rate of conversion.

Consider now the quantum conversion efficiency W (the magnitude which is really measured in the experiment). We see from Eqs. (44) and (46) that the FWM process evolves effectively only for small wave-vector mismatch, $|\Delta k_0| < \beta$. In a real experimental situation, the intensity distribution over the beam transverse cross section is nonuniform. We must account for the fact that Δk_0 and β are both functions of the radial distance ρ. Therefore $\beta(\rho) > |\Delta k_0(\rho)|$ holds for the whole beam cross section only in the case of a passive Kerr medium, i.e., for $|b_{ij}| < \chi$. In this case the quantum conversion efficiency is determined by corresponding curves in Figs. 5 and 6, normalized to the value η.

In the case of an active Kerr medium, $|b_{ij}| \ge \chi$, the quantum conversion efficiency is sharply reduced, since the FWM process evolves effectively only within a small region, where the condition $\beta(\rho) \ge |\Delta k_0(\rho)|$ may hold. The relative area of this region, normalized to the beam area, is denoted as δ. Then the value of the QCE may be estimated by the curves of Figs. 5 and 6, normalized to the value $\delta\bar{\eta}$, where $\bar{\eta}$ is the average value of the local CE $\eta=\eta(\rho)$ in this small pump-beam region.

Now we estimate δ for the case $|b_{ij}| \gg \chi$, supposing that the transverse-intensity distribution of the pump beam has the form (40). The angles θ_j are chosen in such a way that $\Delta k_0(\rho)$ becomes zero at the center of the pump beam. Then, taking into account Eq. (19a), we obtain

$$\delta \sim \frac{\chi\sqrt{I_{10}I_{20}}}{I_{10}(b_{11}+b_{12}-b_{13}-b_{14})+I_{20}(b_{21}+b_{22}-b_{23}-b_{24})} \ll 1\ . \tag{51}$$

It follows from Eqs. (48)–(51) that in the case $|b_{ij}| > \chi$, a high QCE can be achieved if two conditions are simultaneously met: $I_{20} \gg I_{10}$ and $|b_{21}+b_{22}-b_{23}-b_{24}|\sqrt{I_{20}} \ll \chi\sqrt{I_{10}}$. In this case the condition $\beta > |\Delta k_0(\rho)|$ holds over the whole beam cross section, i.e, $\delta \sim 1$. Moreover, the choice of initial wave-vector mismatch in the form of Eq. (37) leads to a local

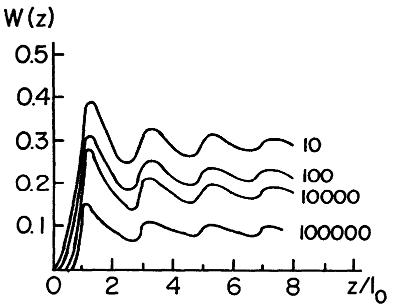

FIG. 7. $W(z)$ dependence in the case $I_{10},I_{20} \gg I_{30}$ for several values of $I_{10}/I_{30}=10,10^2,10^4, \geq 10^5$. The curves correspond to the optimal conditions of Sec. VII.

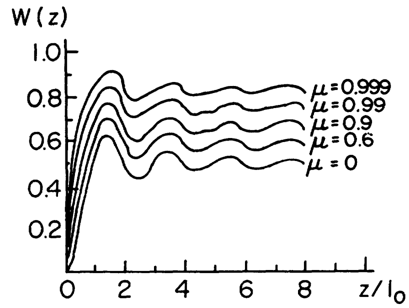

FIG. 8. $W(z)$ dependence in the case $I_{30} \gg I_{10},I_{20}$ for $I_{10}/I_{20}=0$, 0.6, 0.9, 0.99, 0.999.

CE $\eta(\rho)\sim 1$ for the whole beam area. The curves $W(z)$ characterizing this case are shown in Fig. 7. Constructing these curves, we took into account that the parameters μ and ν are coupled by the relation $\nu^{-1}=1-\mu=I_{30}/I_{10}$. It is seen in Fig. 7 that even for the most optimal condition the case $I_{10,20} \gg I_{30}$ is characterized by a relatively low QCE ($W \lesssim 0.3$).

Another opportunity to optimize the conversion process (for $|b_{ij}| \gg \chi$) arises, if the two following conditions hold: $I_{20} \gg I_{10}$ and $\rho_{20} \gg \rho_{10}$, where ρ_{j0} is the radius of beam ω_j. When these conditions simultaneously hold, the variations of $\Delta k_0(\rho)$ over the cross section of beam ω_1 are negligible. Thus, by varying the input beam angles θ_j, one can optimize the fulfillment of Eq. (37), which automatically will extend to the whole ω_1-beam cross section. In this case the CE is maximal and the value $W(z)$ can be estimated according with the corresponding curves of Fig. 7.

VIII. SOLUTION FOR CASE $I_{30} \gg I_{10},I_{20}$

We consider first the case of large ω_3-wave intensity so that $\chi I_{30} \gg (1+\alpha)|\Delta k_0|$. Then we have $S_1=I_{10}$, $S_2=I_{20}$, and $S_3=-I_{30}/(1-\alpha)$. Substituting the values $\nu=0$ and $\mu=I_{10}/I_{20}$ into Eq. (32), we obtain

$$I(z)=I_{10}\mathrm{sn}^2(gz/\mu) , \tag{52}$$

where the amplification rate g is defined as

$$g=\tfrac{1}{2}\chi\sqrt{I_{20}I_{30}} . \tag{53}$$

We should note that the Δk_0 value does not appear in expressions (52) and (53). This means that large values of W can be obtained. Thus, for $I_{10} \lesssim 0.5I_{20}$, expression (52) can be replaced by an approximate $I=I_{10}\sin^2(\pi z/2l)$. Integrating this expression over the pump-beam cross section and taking into account (40), we obtain

$$W(z)=\tfrac{1}{2}+\sin(\pi z/l_0)(4\pi z/l_0) . \tag{54}$$

The $W(z)$ dependence for varying μ parameters is shown in Fig. 8. It is readily seen that the CE increases when $I_{10}\to I_{20}$. We note that Eqs. (52)–(54) and the resulting curves (Fig. 8) are obtained for the optimal case, where the phase-matching condition $\chi I_{30} \gg |\Delta k_0|$ is performed well enough over the entire pump-beam cross section. As follows from (19a), this condition is performed in the case $\chi \gg |b_{31}+b_{32}-b_{33}-b_{34}|$ only. In the opposite case, where $\chi \ll |b_{31}+b_{32}-b_{33}-b_{34}|$, the CE *sharply falls and* W can be estimated using the curves of Fig. 8, with the corrected δ value $\delta\sim\chi/|b_{31}+b_{32}-b_{33}-b_{34}| \ll 1$ (see Sec. VII). In the limit $\chi I_{30} \ll |\Delta k_0|$, Eq. (32) takes the form

$$I(z)=I_{10}(\chi^2 I_{20}I_{30}/\Delta k_0^2)\tanh^2\Delta k_0 z . \tag{55}$$

The FWM evolution in the regime of (55) is characterized by the extremely low local CE ($\eta=\chi^2 I_{20}I_{30}/\Delta k_0^2 \ll 1$). In this case the QCE can be also optimized, if the linear wave-vector mismatch is taken as $\Delta k_L=0$. However, even with such an optimization, the value of W remains very low. Thus, for W_∞ from Eq. (55) with (40), one obtains

$$W_\infty \cong \chi^2 I_{20}/(b_{31}+b_{32}-b_{33}-b_{34})^2 I_{30} \ll 1 . \tag{56}$$

We see from Eqs. (55) and (56) that the parts of the beam cross section where the condition $\chi I_{30} > |\Delta k_0|$ does not hold do not participate in the process of energy conversion. The CE optimization in the case $I_{30} \gg I_{10},I_{20}$ is therefore reduced either to the proper choice of the medium parameters and pump frequencies, for which $\chi > |b_{31}+b_{32}-b_{33}-b_{34}|$, or to the ω_3-beam radius enlarging, in comparison with the radius of the beams $\omega_{1,2}$. In both cases the Δk_0 value exchange over the ω_1-beam cross section becomes negligibly small. If, now, condition (37) is applied, the $W(z)$ dependence is determined by the curves of Fig. 8.

In conclusion, the condition $I_{30} \gg I_{10},I_{20}$ allows use of the nondepleted-pump-beam approach with respect to the ω_3 beam. Therefore expression (52) is equivalent to the corresponding expression of [1], where the three-wave-mixing process has been considered, $\omega_1'+\omega_2'=\omega_3'$.

IX. CONCLUSION

Our analysis of the FWM-process optimization shows that the ideal conditions for effective conversion are sufficiently wide pump beam with uniform intensity distribution over its transverse cross section ($dI_{j0}/d\rho=0$).

Varying the input value of the wave-vector mismatch Δk_0, one can reach the maximal rate of conversion $W \sim 1$. Surprisingly, the intensity-induced Kerr effect does not disturb the optimization procedure. However, there are significant difficulties in obtaining such a beam profile.

A nonuniform beam profile reduces the rate of conversion [see Eq. (40), for example]. Nevertheless, in such conditions the optimization procedure is also possible. The first step of the optimization is to create the condition under which one can neglect the variation of Δk_0 value over the ω_1-beam cross section. Here two approaches are possible. One consists of a choice of the medium parameters or pump frequencies, under which $\chi \gg |b_{21}+b_{22}-b_{23}-b_{24}|$, if the case $I_{20} \gg I_{10} \gg I_{30}$ is considered, or $\chi \gg |b_{31}+b_{32}-b_{33}-b_{34}|$, if $I_{30} \gg I_{10} \geq I_{20}$. Another approach is much simpler. In the case of $I_{20} \gg I_{10} \gg I_{30}(I_{30} \gg I_{20} \geq I_{10})$, it is enough to make the ω_2- (ω_3-) beam radius much wider than the ω_1-beam radius. Then the exchange of Δk_0 over the ω_1-beam cross section will be negligibly small. The second step of optimization is reduced to variation of the Δk_0 value in accordance with the optimization requirement (37).

The above analysis is for near-ideal conditions. One should note that phenomena such as pump divergency, its time limitation, and nonuniform medium, which would lead to some reduction of the QCE and to $W(z)$ oscillation smoothing, were not taken into account. Consequently, the transverse-intensity distribution will also be smoothed (see Fig. 4). We should note also that the transverse-field-profile influence is considered in the simpliest way in order to be able to analyze the solutions. A more proper approach is based on including the perpendicular derivatives [30,31].

The formulation developed here is used for a successful description of various types of FWM processes. Thus, after a trivial transformation, Eqs. (21) and (26) describe the third-harmonic-generation process $\omega_4 = \omega_1 + \omega_2 + \omega_3$. A similar formalism can be used in the case of resonant interaction with atomic vapors. In this case expansion (1) is not valid and the Hamiltonian of the system should be represented by $N\hbar\Omega$, where N is the medium density and Ω is the quasienergy of a dressed atom (or molecule) in an external field, that is, the Stark shift of an atomic ground state [32,33].

The theory developed here has a very wide field of application. First of all, it includes any short-pulsed-wave interaction through the medium $\chi^{(3)}$ susceptibility either in the gas or solid phase or propagational effects in waveguides and fibers, etc. Recently, one of authors (B.G.) has started a study of the optimization of third-harmonic-generation (THG) conversion in an alkali-metal vapor. The dramatic increase of THG efficiency (up to 60%) is based on the predictions of our theory, allowing one to eliminate the negative influence of the optical Kerr effect known as a most severe effect limiting the growth of conversion. More detailed theoretical calculations are on the way.

In conclusion, we note that Eq. (21) and all preceding expressions are still valid, when the linear refractive indices $n(\omega_j)$ are strongly distinguished from unity. This case is reduced to that considered above by simple substitution: $q \rightarrow \Delta k_L$ and $I_j \rightarrow I_j = \mathrm{cn}(\omega_j)|E_j|^2 \cos Q_j / 2\pi\hbar\omega_j$.

ACKNOWLEDGMENTS

The authors wish to thank Professor M. L. Ter-Mikaelyan for useful discussions.

[1] J. A. Armstrong, N. Bloembergen, J. Ducuing, and P. S. Pershan, Phys. Rev. **127**, 1918 (1962).

[2] P. A. Apanasevich and A. A. Afanasiev, Opt. Spektrosk. **33**, 300 (1972).

[3] D. Harter, P. Narum, N. J. Raymer, and R. W. Boyd, Phys. Rev. Lett. **46**, 1192 (1981); Phys. Rev. A **24**, 411 (1981); D. J. Harter and R. W. Boyd, *ibid.* **29**, 739 (1984).

[4] V. M. Arutyunyan, E. G. Kanetsyan, and V. O. Chaltikyan, Zh. Eksp. Teor. Fiz. **59**, 195 (1970) [Sov. Phys.—JETP **32**, 108 (1971)].

[5] A. M. Plekhanov, S. G. Rautian, V. P. Safanov, and V. M. Chernobrod, Zh. Eksp. Teor. Fiz. **88**, 426 (1985) [Sov. Phys.—JETP **61**, 249 (1985)].

[6] A. Elci, D. Rogovin, D. Depatie, and D. Haucissen, J. Opt. Soc. Am. **70**, 990 (1980).

[7] Y. Prior, A. Bogdan, N. Dagenais, and N. Bleombergen, Phys. Rev. A **46**, 111 (1981).

[8] A. M. Levin, N. Chencinsky, W. M. Schreiber, A. N. Weiszmann, and Y. Prior, Phys. Rev. A **35**, 2550 (1987).

[9] T. A. deTample, M. K. Guznick, and F. H. Jabien, Phys. Rev. A **37**, 3358 (1988).

[10] B. V. Kryzhanovsky, Kvant. Elektron. (Moscow) **14**, 2209 (1987) [Sov. J. Quantum Electron. **17**, 1407 (1987)]; **16**, 281 (1989) [**19**, 185 (1991)]; Opt. Spektrosk. **59**, 167 (1985) [Opt. Spectrosc. (U.S.S.R) **59**, 98 (1985)]; **63**, 154 (1987) [**63**, 90 (1987)].

[11] M. E. Grenshaw and C. D. Cantrell, Phys. Rev. A **39**, 126 (1989).

[12] N. Bloembergen, *Nonlinear Optics* (Benjamin, New York, 1965).

[13] C. A. Akhmanov and R. V. Khokhlov, *Nonlinear Optics Problems* (VINITI, Moscow, 1964).

[14] Y. R. Shen, *The Principles of Nonlinear Optics* (Wiley, New York, 1984).

[15] Y. Chen and A. Snyder, Opt. Lett. **14**, 87 (1989); Y. Chen, J. Opt. Soc. Am. B **6**, 1986 (1989).

[16] C. J. McKinstrie and G. G. Luther, Phys. Lett. A **127**, 14 (1988); C. J. McKinstrie, G. G. Luther, and S. M. Batha, J. Opt. Soc. Am. B **7**, 340 (1990).

[17] G. Cappellini and S. Trillo, J. Opt. Soc. Am. B **8**, 824 (1991).

[18] A. O. Melikyan and S. G. Saakyan, Zh. Eksp. Teor. Fiz. **76**, 1530 (1979) [Sov. Phys—JETP **49**, 776 (1979)].

[19] B. V. Kryzhanovsky and A. R. Karapetyan, Zh. Eksp. Teor. Fiz. **99**, 1103 (1991) [Sov. Phys.—JETP **72**, 613 (1991)]; B. V. Kryzhanovsky, A. R. Karapetyan, and B.

Glushko, Phys. Rev. A **44**, 6036 (1991).

[20] L. D. Landau and E. M. Lifshitz, *Electrodynamics of Continuous Media* (Nauka, Moscow, 1964).

[21] H. A. House, IRE Trans. Microwave Theory Tech. **6**, 317 (1958).

[22] W. H. Louisell, *Coupled Mode and Parametric Electronics* (Wiley, New York, 1960).

[23] H. Bateman and A. Erdelyi, *Higher Transcendental Functions* (Publisher, City, 1955), Vol. 3.

[24] N. I. Akhiezer, *Elements of Elliptical Functions Theory* (Nauka, Moscow, 1970).

[25] E. T. Whittaker and G. N. Watson, *A Course of Modern Analysis* (Cambridge University Press, New York, 1927).

[26] E. Jahnke, F. Emde, and F. Losch, *Tables of Functions* (McGraw-Hill, New York, 1960).

[27] *Handbook of Mathematical Functions,* edited by M. Abramowitz and I. A. Stegun (Dover, New York, 1964).

[28] F. G. Tricomi, *Funciony Ellyptische* (Zanichelli, Bologna, 1951).

[29] V. V. Krasnikov, M. S. Pshenichnikov, and V. S. Salomatin, Opt. Spektrosk. **62**, 10 (1987) [Opt. Spectrosc. (U.S.S.R.) **62**, 6 (1987)].

[30] V. V. Eliseev, V. T. Tikhonchuk, and A. A. Zozulya, J. Opt. Soc. Am. B **7**, 2174 (1990).

[31] R. H. Lehmberg and K. A. Holder, Phys. Rev. A **22**, 2156 (1980).

[32] M. L. Ter-Mikaelyan and A. O. Melikyan, Zh. Eksp. Teor. Fiz. **58**, 281 (1970) [Sov. Phys.—JETP **31**, 153 (1970)].

[33] A. O. Melikyan, Kvant. Elektron. (Moscow) **4**, 429 (1977) [Sov. J. Quantum Electron. **7**, 237 (1977)].